10.2478/v10048-011-0001-6

MEASUREMENT SCIENCE REVIEW, Volume 11, No. 1, 2011

Synthesis and Transport Properties of Nanostructured VO_2 by Mechanochemical Processing

P. Billik[1,2], M. Čaplovičová[3], J. Maňka[1], Ľ. Čaplovič[4], A. Cigáň[1], A. Koňakovský[1], R. Bystrický[1], A. Dvurečenskij[1]

[1]Institute of Measurement Science, Slovak Academy of Sciences, Dúbravská cesta 9, 841 04 Bratislava, Slovakia
e-mail: peter.billik@savba.sk

[2]Department of Inorganic Chemistry, Faculty of Natural Sciences, Comenius University, Mlynská dolina, 842 15 Bratislava, Slovakia

[3]Department of Geology of Mineral Deposits, Faculty of Natural Sciences, Comenius University, Mlynská dolina, 842 15 Bratislava, Slovakia

[4]Institute of Materials Science, Faculty of Materials Science and Technology, J. Bottu 25, 917 24 Trnava, Slovakia

The high-energy milling of the V_2O_5-Na_2SO_3 mixture in the range of 5 - 100 min leads to a synthesis of monoclinic VO_2. The starting and minimum (at 220 °C) values of electric resistance *R* of the 100 min milled and pressed VO_2-Na_2SO_4 mixture were 13.9 MΩ and 91.5 kΩ, respectively. The subsequent washing of the as-milled powder partially leads to the development of VO_2 nanostructures with tube-like, sheet-like and rod-like morphology, besides VO_2 (B) belt-like morphology, depending on the milling times.

Keywords: Nanostructures, chemical synthesis, transmission electron microscopy (TEM), electrical resistivity

1. Introduction

A PROMINENT OXIDE VO_2 is represented due to its extremely interesting physical and chemical properties.

Depending on its primary particle size, VO_2 undergoes a reversible first order phase transition at ~68 °C [1]. Above the phase transition, VO_2 has a tetragonal rutile structure, while the low temperature phase is monoclinic. The monoclinic to rutile phase transition is followed by up to ~10^5 decrease in electrical resistivity as well as a large change in transparency in the infrared region [1-5]. This makes VO_2 a promising material for applications such as thermal sensors, smart IR optical windows, emissive coatings [1-5] or thermochromic pigments [6]. In addition, the wide range of oxidation states of vanadium from +2 to +5 may accommodate multi-electron transfer processes with applications in rechargeable lithium batteries [7]. New lithium batteries using VO_2 (B) as an example of attractive electrode material with a layered structure, exhibit a reversible specific capacity exceeding 300 mAh/g [8]. Nowadays, a new cubic crystal structure for VO_2 nanorods with a large optical band gap of 2.7 eV has been reported by Wang et al., which surprisingly shows excellent photocatalytic activity in hydrogen production and shows good field emission properties [2, 5]. The recently observed rate of publications based on the new morphology of VO_2, including one-dimensional (1D) nanostructures such as nanorods [9], nanoribbons [10], nanobelts [8, 11], nanowires [12] or two dimensional (2D) lamellar or sheet-like nanostructures [7, 13-15], is demonstrating that the unusual morphology based on the VO_2 system is a rule rather than an exception. Unfortunately, the attractive synthesis of nanostructured VO_2 with unusual properties requires a relatively complicated process control and in many cases, time consuming hydrothermal conditions are required [7-10, 12, 14, 15]. In this regard, it is still a challenge to develop low-cost routes for the synthesis of VO_2 nanomaterials on a large scale.

In recent times, high-energy ball milling has been widely applied for the synthesis of nanocrystalline powders, with a significant potential for a large-scale production. High energy milling of precursor powders leads to the formation of a nanoscale composite structure, which reacts during milling to form a mixture of separated nanocrystals of the desired phase within a soluble salt matrix, which is removed by water washing [16-19]. Herein, we report a facile mechanochemical synthesis of nanostructured VO_2.

2. Material & Methods

Mechanochemical synthesis was performed in the high-energy planetary mill, TB-2 (Kadaň Ltd., Slovakia) at 890 rpm, with the power input of 3.0 kW. 10 g of a starting mixture corresponding to a V_2O_5/Na_2SO_3 molar ratio of 1:2 was loaded to corundum jars of the 0.2 dm^3 inner volume. Yttrium stabilized ZrO_2 (YTZ, Tosoh, Japan) ceramic balls with 10 mm diameter were used as the milling media. The weight ratio between the balls and the powder mixture was 20:1. The milling was interrupted at different times to remove the powder for an analysis using X-ray diffraction (Philips PW 1050 diffractometer, Cu-Kα radiation). The salt matrix by-product was then removed by washing with water. The washed powders were dried at 120 °C for 2 h in air. The average crystallite size was calculated from diffraction peak broadening using the Sherrer equation in the form reported in [3]. The morphology of the powder obtained after the washing procedure was examined in a JEOL FX 2000 transmission electron microscope (TEM). For the

measurement of temperature dependences of the electric resistance *R*, the 100 min milled powders were pressed into pellets by using a 200 MPa press. A silver paste, RITE-LOCK SL69 (0.5 mΩ/cm), was used for contacting the sample. The temperature was measured by a platinum sensor, PT-103 from Lakeshore. The temperature measurement uncertainty was smaller than 50 mK. An electric oven was used for the sample temperature regulation in the range of 25-220 °C. An electronic switch was used to measure the current and voltage of the sensor and sample by the FLUKE 8846A multimeter. Resistance values were determined as a ratio of the electric voltage on the sample and electric current flowing through the sample driven by DC voltage of 9 V (with the internal resistance of 10 kΩ). Repeated measurements over time showed that the sample's room temperature resistance had a strong tendency to decrease - more than a one order decrease during about one and a half month.

3. Results and discussion

Fig.1 shows the XRD patterns of the starting material and as-milled powders between 2 and 100 min. The diffraction peaks of the reactants completely disappear after 20 min milling, however, very broad peaks corresponding to the low-crystalline monoclinic VO_2 (ICDD Card No. 44-0252) and Na_2SO_4 are visible after milling for 5 min only, (c) pattern in Fig.1.

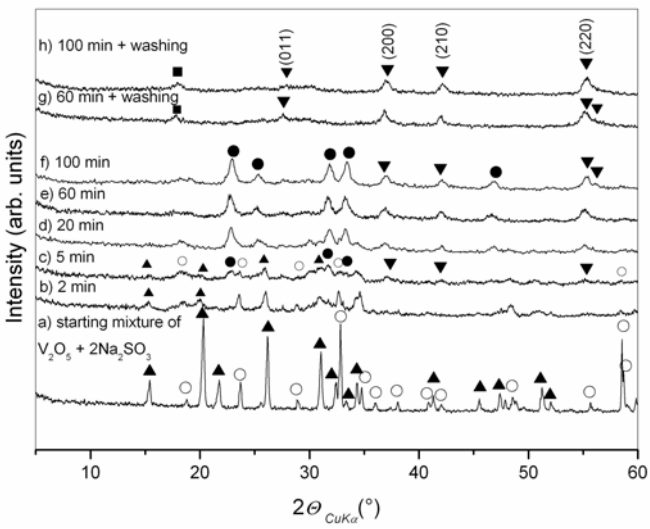

Fig.1. XRD patterns of the starting V_2O_5 + $2Na_2SO_3$ mixture (a), and powders milled between 2 and 100 min (b-h). (▲): V_2O_5, (▼): VO_2, (○): Na_2SO_3, (●): Na_2SO_4, (■): $VO_2{\cdot}xH_2O$.

Interestingly, the peaks corresponding to the excessive Na_2SO_3 phase are absent from the pattern. This might be due to the fact that the Na_2SO_3 phase exists in an amorphous state and/or Na_2SO_3 undergoes the oxidation with air to Na_2SO_4 during milling. In this case, the following reaction can be proposed for the process:

$$V_2O_5 + 2Na_2SO_3 + 1/2O_2 \rightarrow 2VO_2 + 2Na_2SO_4 \qquad \Delta G^\circ_{298\,K} = -439 \text{ kJ mol}^{-1} \qquad (1)$$

The colour of the product changed from yellow ochre (V_2O_5) to dark green after 5 min, which indicated that V^{5+} were partially reduced to V^{4+} cations. After the next prolongation of the milling time (20 min), the colour turned into black, which indicated that V^{5+}cations had been reduced to V^{4+} cations [10]. With increasing the milling time from 20 to 100 min, the crystallization process of VO_2 and Na_2SO_4 is more apparent. The crystallite size of VO_2 and Na_2SO_4, as calculated from diffraction peak broadening, increased from ~9 nm to 13 nm in the case of VO_2, and from 17 nm to ~ 20 nm in the case of Na_2SO_4 after 20 min and 100 min milling.

The crystallization phenomena involved local atomic displacements associated with the large local strain, temperature and pressure rise, which allows decomposition of the metastable amorphous phase, resulting in subsequent nucleation and grain growth [20–22]. Comparable mechanochemically induced crystallisations of amorphous Mn_2O_3 and SnO_2 were reported previously in our earlier studies [18, 19].

The results of the electrical measurements performed on the 100 min milled sample are reported in Fig.2. The starting (at 25 °C) and minimum (at 220 °C) values of *R* are 13.9 MΩ and 91.5 kΩ, respectively. It means that the ratio of the resistance values is about 150. We can see that the resistance of compacted samples undergoes a strong temperature dependence, typical for semiconductor to metal phase transformation of monoclinic VO_2 [1, 3]. However, the obtained resistance values at 150 °C are still atypically high. As the salt matrix of Na_2SO_4 was present in the compacted samples in the high volume fraction (~ 55 vol. %), we suppose that the relatively high resistivity could have been caused by the presence of the Na_2SO_4 matrix. Moreover, the significant differences in *R* and hysteresis loops observed during the repeated temperature cycling (not shown herein) and a broad temperature transition indicate other possible effects connected with a non-uniform crystallite size distribution, absorbed water or high stress state of nanoparticles in milled and compacted powders [1, 28].

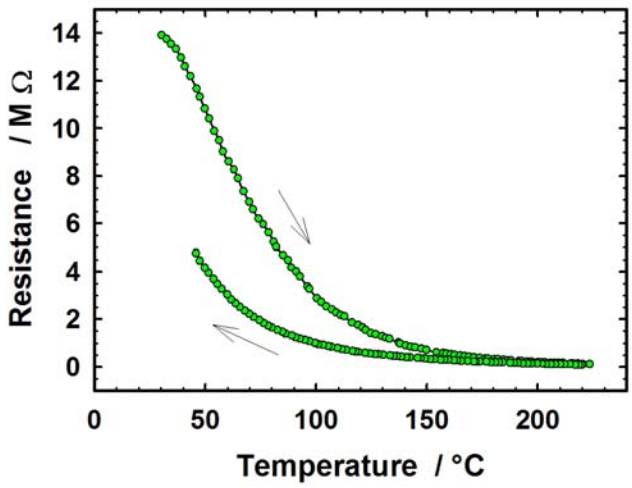

Fig.2. *R* vs. *T* dependence of the 100 min milled and by 200 MPa pressed sample. (The arrows show the increase and following decrease of temperature).

Fig.3 (a) shows the TEM microstructural studies of VO_2 powder formed upon milling for 100 min, followed by the washing procedure. The powder is composed from large aggregates of primary and non-uniform VO_2 nanoparticles. Fig.3 (b) shows the same sample obtained at higher magnification, and non-spherical particles of VO_2 with TEM sizes in the range of 10–20 nm are visible. It can be concluded that the TEM image of the sample obtained after 100 min milling shows aggregates of VO_2 typical for the high-energy ball milling procedure. However, the careful TEM analysis shows sample areas with unexpected new morphological changes in the samples.

TEM images of nanostructures formed upon milling for 5, 20, 60 and 100 min, followed by the washing procedure, are shown in Fig.4. Beside grained VO_2 aggregates revealed in as-milled samples for 100 min, Fig.3 (a,b) and 4 (d), TEM results show the partial formation of nanorods with the width of 8-25 nm and lengths up to 500 nm, Fig.4 (a), (f). As it can be seen from Fig.4 (c–f), with prolonged milling time (60 and 100 min) followed by washing, the new lamellar, sheet-like and tube-like nanostructures were observed in the samples, which demonstrates that the milling time influences the chemical interaction of mechanochemically formed VO_2 with water during the subsequent washing treatment.

This observation is also partially supported by XRD, Fig.1(g), (h), where the samples milled for 60 and 100 min and subsequently washed show new reflections, most probably $VO_2{\cdot}xH_2O$. Due to the washing procedure the diffractions, which belong to the Na_2SO_4 salt matrix, are absent from the pattern. The structure determination based on this XRD pattern is impossible, because there are too few and broad diffractions. Therefore, the exact structure determination was performed by the selected area electron diffraction (SAED) method. SAED pattern in inset in Fig.4 (e) recorded from arrowed belt-like structure can be indexed as a metastable monoclinic VO_2 (B) with the following parameters: a = 1.2093 nm, b = 0.3702 nm, c = 0.6433 nm and β = 106.97° according to JCPDS 81-2392. Growth direction is [010]. Hence, the formation of very fine lamellar 1D and 2D nanostructures directly during high-energy ball milling can be excluded. We suppose that the washing procedure and high reactivity of new-formed VO_2 nanopowders with water play a key role in the new morphology evolution.

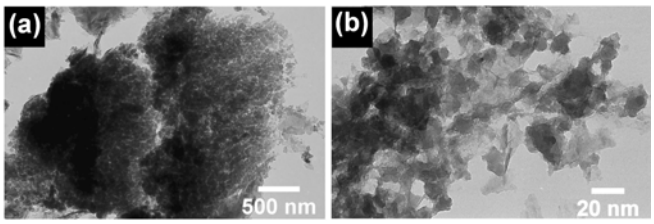

Fig.3. TEM images of VO_2 obtained mechanochemically by milling of the V_2O_5 + 2 Na_2SO_3 mixture for 100 min after the subsequent washing procedure.

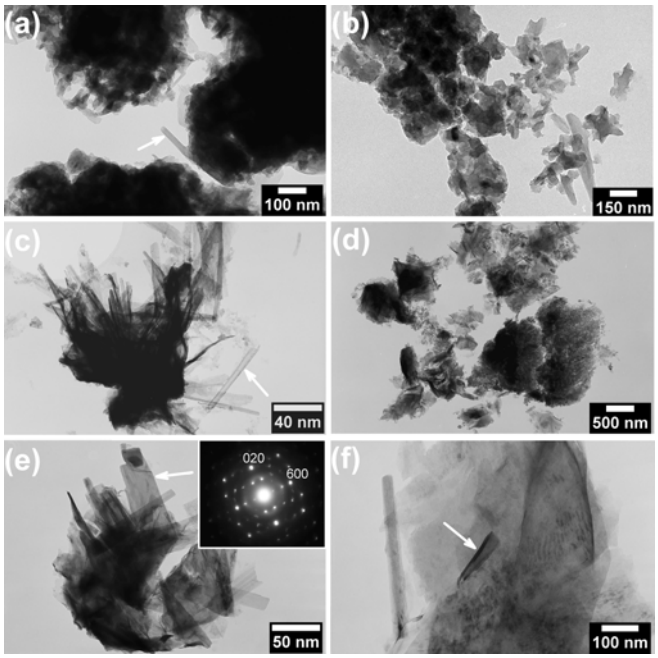

Fig.4. TEM images of VO_2 obtained by milling of the V_2O_5 + 2 Na_2SO_3 mixture for 5 min (a), 20 min (b), 60 min (c) and 100 min (d-f) after the subsequent washing procedure.

Beside VO_2 (B) [8], many metastable and hydrated VO_2 phases, such as $V_2O_4{\cdot}0.25H_2O$ [12], $V_2O_4{\cdot}2H_2O$ [13], $VO_{1.75}(OH)_{0.25}$ [14] and $VO_2{\cdot}0.5H_2O$ [24] are composed of a layered crystal structure. According to these facts, the hydrating-exfoliating-splitting mechanism may play a key role in the formation of 1D and 2D structures [12, 25]. Previously, this mechanism has been used to explain the growth of different 1D and 2D nanostructures based on the layered precursors of VO_2 [12, 14], TiO_2 [25] and MnO_2 [23] prepared under hydrothermal conditions. Nevertheless, it has been demonstrated that the 1D and 2D nanostructures can be formed under non-hydrothermal conditions effectively. For example, Manivannan et al. [26] observed the self-assembly of spherical particles of $MnV_2O_6{\cdot}4H_2O$ with a layered structure prepared mechanochemically into nanorods or nanobelts during the simple washing and Liu et al. [27] observed the formation of β-MnO_2 nanorods by the simple refluxing process of layered δ-MnO_2, which grow from the amorphous MnO_2. In the same way, we believe that the as-milled and very reactive VO_2 powders are transformed to the layered and metastable phases of VO_2 (B) or $VO_2{\cdot}xH_2O$, in which H_2O molecules occupy the interlayer spaces. Therefore, interactions between the layers are weakened. However, this structure is unstable during washing and the layers are gradually exfoliated to form asymmetric nanosheets, Fig.4 (f). An intrinsic tension exists that might gradually, in some cases, roll up edges of the nanosheets [12, 14, 23, 25, 26] and the tube-like morphology can be obtained, arrowed in Fig.4 (f). In order to release the next strong stress and lower the total energy, the nanosheets are split, resulting in the partial formation of rod-like morphology, Fig.4(f).

Thus, the washing treatment plays a crucial role in the evolution of nanostructured VO_2 powders.

4. Conclusion

In summary, the mechanochemical treatment of V_2O_5 + 2 Na_2SO_3 mixture for 5-100 min leads to the formation of nanocrystalline VO_2 with XRD particle size in the range of 9-13 nm. A prolonged mechanochemical treatment enhances the crystallization process of VO_2. The resistance of the compacted 100 min milled sample shows a strong temperature dependence, typically accompanying semiconductor to metal phase transformation of monoclinic VO_2. The elimination of Na_2SO_4 salt matrix with the simple washing procedure partially leads to the reaction of VO_2 with water and new VO_2 phases with a unique 1D and 2D morphology were obtained. This mechanochemical method can be easily adjusted to prepare VO_2 nanopowders on a large scale.

Acknowledgement

This work was supported by the Agency of the Ministry of Education of the Slovak Republic for the Structural Funds of the EU, Operational Programme Research and Development, Project Codes 26240120011 and 26220120014, and by VEGA grants 2/0160/10 and 2/0020/11. The authors wish to thank Kadaň Ltd. Slovakia for the support in the construction of the planetary mill TB-2.

References

[1] Lopez, R., Haynes, T.E., Boatner, L.A., Feldman, L.C., Haglund Jr., R.F. (2002). Size effects in the structural phase transition of VO_2 nanoparticles. *Phys. Rev. B,* 65 (22), 2241131-2241135.

[2] Wang, Y., Zhang, Z. (2009). Synthesis and field emission property of VO_2 nanorods with a body-centered-cubic structure. *Physica E,* 41 (4), 548-551.

[3] Guinneton, F., Sauques, L., Valmalette, J.C., Cros, F., Gavarri, J.R. (2001). Comparative study between nanocrystalline powder and thin film of vanadium dioxide: Electrical and infrared properties. *J. Phys. Chem. Solids,* 62 (7), 1229-1238.

[4] Eyert, V. (2002). The metal-insulator transitions of VO_2: A band theoretical approach. *Ann. Phys.,* 11 (9), 650-702.

[5] Wang, Y., Zhang, Z., Zhu, Y., Li, Z., Vajtai, R., Ci, L., Ajayan, P.M. (2008). Nanostructured VO_2 photo-catalysts for hydrogen production. *ACS Nano,* 2 (7), 1492-1496.

[6] Bai, H., Cortie, M.B., Maaroof, A.I., Dowd, A., Kealley, C., Smith, G.B. (2009). The preparation of a plasmonically resonant VO_2 thermochromic pigment. *Nanotechnology,* 20 (8), 085607.

[7] Ding, N., Feng, X., Liu, S., Xu, J., Fang, X., Lieberwirth, I., Chen, C. (2009). High capacity and excellent cyclability of vanadium (IV) oxide in lithium battery applications. *Electrochem. Commun.,* 11 (3), 538-541.

[8] Liu, J., Li, Q., Wang, T., Yu, D., Li, Y. (2004). Metastable vanadium dioxide nanobelts: Hydro-thermal synthesis, electrical transport, and magnetic properties. *Angew. Chem. Int. Ed.,* 43 (38), 5048-5052.

[9] Chen, W., Peng, J., Mai, L., Yu, H., Qi, Y. (2004). Synthesis and characterization of novel vanadium dioxide nanorods. *Solid State Commun.,* 132 (8), 513-516.

[10] Kong, L., Liu, Z., Shao, M., Xie, Q., Yu, W., Qian, Y. (2004). Controlled synthesis of single-crystal $VO_x{\cdot}nH_2O$ nanoribbons via a hydrothermal reduction method. *J. Solid State Chem.,* 177 (3), 690-695.

[11] Li, G., Chao, K., Peng, H., Chen, K., Zhang, Z. (2007). Low-valent vanadium oxide nanostructures with controlled crystal structures and morphologies. *Inorg. Chem.,* 46 (14), 5787-5790.

[12] Wei, M., Sugihara, H., Honma, I., Ichihara, M., Zhou, H. (2005). A new metastable phase of crystallized $V_2O_4{\cdot}0.25H_2O$ nanowires: Synthesis and electro-chemical measurements. *Adv. Mater.,* 17 (24), 2964-2969.

[13] Bai, L., Gao, Y., Li, W., Luo, H., Jin, P. (2008). Synthesis and atmospheric instability of well crystallized rod-shaped $V_2O_4{\cdot}2H_2O$ powders prepared in an aqueous solution. *J. Ceram. Soc. Jpn.,* 116 (1351), 395-399.

[14] Wei, M., Qi, Z., Ichihara, M., Hirabayashi, M., Honma, I., Zhou, H. (2006). Synthesis of single-crystal vanadium dioxide nanosheets by the hydrothermal process. *J. Crys. Growth.,* 296 (1), 1-5.

[15] Whittaker, L., Zhang, H., Banerjee, S. (2009). VO_2 nanosheets exhibiting a well-defined metal-insulator phase transition. *J. Mater. Chem.,* 19 (19), 2968-2974.

[16] Godočíková, E., Baláž, P., Gock, E., Choi, W.S., Kim, B.S. (2006). Mechanochemical synthesis of the nanocrystalline semiconductors in an industrial mill. *Powder Technol.,* 164 (3), 147-152.

[17] Dodd, A.C., McCormick, P.G. (2001). Synthesis of nanoparticulate zirconia by mechanochemical processing. *Scr. Mater.,* 44 (8-9), 1725-1729.

[18] Billik, P., Čaplovičová, M., Janata, J., Fajnor, V.Š (2008). Direct synthesis of nanocrystalline, spherical α-Mn_2O_3 particles by mechanochemical reduction. *Mater. Lett.,* 62 (6-7), 1052-1054.

[19] Billik, P., Čaplovičová, M. (2009). Synthesis of nanocrystalline SnO_2 powder from $SnCl_4$ by mecha-nochemical processing. *Powder Technol.,* 191 (3), 235-239.

[20] Trudeau, M.L., Schulz, R., Dussault, D., Van Neste, A. (1990). Structural changes during high-energy ball milling of iron-based amorphous alloys: Is high-energy ball milling equivalent to a thermal process? *Phys. Rev. Lett.,* 64 (1), 99-102.

[21] Koch, C.C. (1997). Synthesis of nanostructured materials by mechanical milling: Problems and opportunities. *Nanostruc. Mater.,* 9 (1-8), 13-22.

[22] Huang, B., Perez, R.J., Crawford, P.J., Sharif, A.A., Nutt, S.R., Lavernia, E.J. (1995). Mechanically induced crystallization of metglas $Fe_{78}B_{13}Si_9$ during cryogenic high energy ball milling. *Nanostruct. Mater.,* 5 (5), 545-553.

[23] Wang, X., Li, Y. (2003). Synthesis and formation mechanism of manganese dioxide nanowires/nanorods. *Chem.-Eur. J.,* 9 (1), 300-306.

[24] Hagrman, D., Zubieta, J., Warren, C.J., Meyer, L.M., Treacy, M.M.J., Haushalter, R.C. (1998) A new polymorph of VO_2 prepared by soft chemical methods. *J. Solid State Chem.,* 138 (1), 178-182.

[25] Wei, M., Konishi, Y., Zhou, H., Sugihara, H., Arakawa, H. (2004). A simple method to synthesize nanowires titanium dioxide from layered titanate particles. *Chem. Phys. Lett.,* 400 (1-3), 231-234.

[26] Manivannan, V., Parhi, P., Howard, J. (2008). Mechanochemical metathesis synthesis and characterrization of nano-structured $MnV_2O_6 \cdot xH_2O$ (x = 2, 4). *J. Cryst. Growth,* 310 (11), 2793-2799.

[27] Liu, X., Fu, S., Huang, C. (2005). Synthesis, characterization and magnetic properties of β-MnO_2 nanorods. *Powder Technol.,* 154 (2-3), 120-124.

[28] Cao, J., Wu, J. (2011). Strain effects in low-dimensional transition metal oxides. *Mater. Sci. Eng.-Reports,* 71 (2-4), 35-52.

Received January 24, 2011.
Accepted March 22, 2011.